AD-A099 719 JAYCOR ALEXANDRIA VA F/G 20/9
ELECTRON HEATING IN STRONGLY BEADED HIGH-Z PINCH DISCHARGES AT --ETC(U)
MAY 81 J GUILLORY DNA001-79-C-0189
UNCLASSIFIED JAYCOR-J207-81-003 NL

END
DATE
FILMED
6-81
DTIC

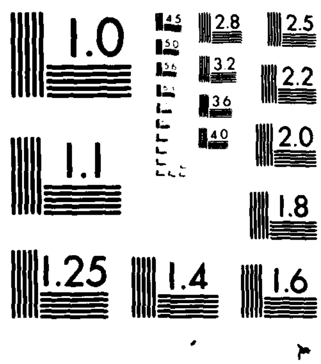

MICROCOPY RESOLUTION TEST CHART

LEVEL II

AD A099719

JAYCOR

DTIC
ELECTE
JUN 4 1981
S D
A

DTIC FILE COPY

81 6 04 056

205 South Whiting Street
Alexandria, Virginia 22304

12) 241

6) ELECTRON HEATING IN STRONGLY BEADED
HIGH-Z PINCH DISCHARGES AT
HIGH DENSITIES.

10 J. Guillory

11) May 1981

9) Technical rept.

JAYCOR Tech Report No.
14) JAYCOR-J207-81-003

Prepared under JAYCOR Contract
13) DNA001-79-C-0189

for

Defense Nuclear Agency

DTIC
S ELECTE D
JUN 4 1981
A

39...

CONTENTS

INTRODUCTION

The late-time, fully-developed stage of sausage-like "beading" of z-pinch discharges can give rise to enhanced electron heating (and thus enhanced radiative losses), caused by Ohmic anomalous heating in the constricted regions. In this report, this transfer of energy from condensations of magnetic field energy to radiation is examined quantitatively, based on a simplified dynamical model for the nonlinear instability driving terms.

Constricted portions of the discharge, with low density and cross-section, and mostly or entirely "anomalous" current, alternate with the higher density "beads", which carry current classically. The extreme limit of this phenomenon is that of multiple diodes in series, with the nearly-evacuated low density regions considered as bipolar-flow diodes, with pinched electron flow, ~~as suggested by Goldstein (1978)~~. In all probability, the low-density regions cannot evacuate to the extent required for such vacuum-diode behavior.

The overall resistive heating rate is of course VI, with the total current I given by appropriate circuit equations, but the local heating rates for electrons in the low density regions are balanced by increased radiative loss when these hotter electrons collide with the denser blobs of plasma. The blobs cannot respond hydrodynamically to the increased heating before radiation loses the deposited energy.

CURRENT

We first examine the conditions under which all the current in the low-density regions would be drift-speed limited, i.e., (approximately) when the classical drift speed $v_d = \sigma E/n_e e$ would exceed the sound speed c_s. From $\sigma_\perp = \omega_p^2/4\pi\nu_{ei}$ and

$$\nu_{ei}(\sec^{-1}) = 0.9 \times 10^{11} \left(\frac{\ell n\Lambda}{10}\right) \left(\frac{z}{10}\right)^2 \left(\frac{n_i}{10^{18}}\right) T_{keV}^{-3/2} \qquad (1)$$

we get

$$v_d(\text{cm/s}) = 1.8 \times 10^{10} \left(\frac{10}{\ell n\Lambda}\right) \left(\frac{10}{z}\right)^2 \left(\frac{10^{18}}{n_i}\right) T_{keV}^{3/2}\, E(\text{MV/cm}) \qquad (2)$$

where z is the degree of ionization ($n_e = zn_i$), $\sigma_\perp$ is the axial conductivity, (across magnetic field lines) and $\ell n\Lambda$ is the plasma parameter. The classical drift speed rises rapidly with T as the plasma becomes less collisional.

This is to be compared with

$$c_s = 2.24 \times 10^7 \left(\frac{26}{A}\ \frac{z}{10}\right)^{1/2} T_{keV}^{1/2} \ . \qquad (3)$$

For 10-times ionized aluminum (A = 26, z = 10), one sees that with electrons at keV temperatures the classical drift speed greatly exceeds the sound speed for MV/cm fields unless n_i is of order 10^{21} cm^{-3} or greater. Elsewhere we argue that the actual drift speed cannot much exceed the sound speed, so that the current is drift-speed limited to a value approximately

$$I_a(\text{MA}) = 0.36 \left(\frac{26}{A}\right)^{1/2} \left(\frac{z}{10}\right)^{3/2} \left(\frac{n_i}{10^{18}}\right) T_{keV}^{1/2} \left(\frac{\pi r_a^2}{1\ \text{mm}^2}\right) \qquad (4)$$

in the anomalous ("a") low-density regions of cross-sectional area πr_a^2. *Since the current density is divergenceless, this must be the current in the circuit.*

VOLTAGE DROP IN LOW DENSITY REGIONS

We now envision a number N of such millimeter size low-density "anomalous" regions of length ℓ_a alternating with denser "classical" regions ("beads") of length ℓ_c. Each "classical" region has, in general, a core which carries no current because it has not been penetrated by the magnetic field (and hence has no inductive E), a classical skin current layer, and an "anomalous" (drift-speed limited) outer corona. The electrical load is thus envisioned as a transmission line consisting of N elements in series, with each element as in figure 1. Since the total current is divergenceless, it is given by Eq. (4), and depends on the applied voltage only through the temperature. If the corona carries only a small fraction (1-β<<1) of the current, the DC voltage drop along each classical bead is $R_c I$ where R_c is the classical resistance of the bead,

$$R_c = \frac{\ell_c}{\pi(r_c^2 - r_i^2)\sigma}$$

$$\text{i.e. } R_c(\Omega) = 3.5 \times 10^{-4} \left(\frac{z}{10}\right)\left(\frac{\ell n\Lambda}{10}\right) \frac{\ell_c(\text{mm})}{\pi(r_c^2 - r_i^2)(\text{mm}^2)} T_{\text{keV}}^{-3/2} \qquad (5)$$

with r_c the bead radius and $r_i (< r_c)$ the current penetration radius.

One can see that when inductive ($L\dot{I}$ and $\dot{L}I$) effects are small (i.e., if $\dot{L} \approx 0$ when I peaks or dips), the classical resistance of a few tens of 1 mm beads at roughly 1 keV is quite small if the current penetrates the beads, and almost all the voltage drop occurs in the anomalous regions. On the other hand, r_i/r_c tends to be frozen in at early times by the formation of the high conductivity, and tends to have values of order 10^{-1} or less, so the resistance is larger than the current-penetrated value by an order of magnitude or more. Still, this gives only a small resistance for the "classical" portion of the circuit and most of the DC voltage drop would occur in the anomalous regions.

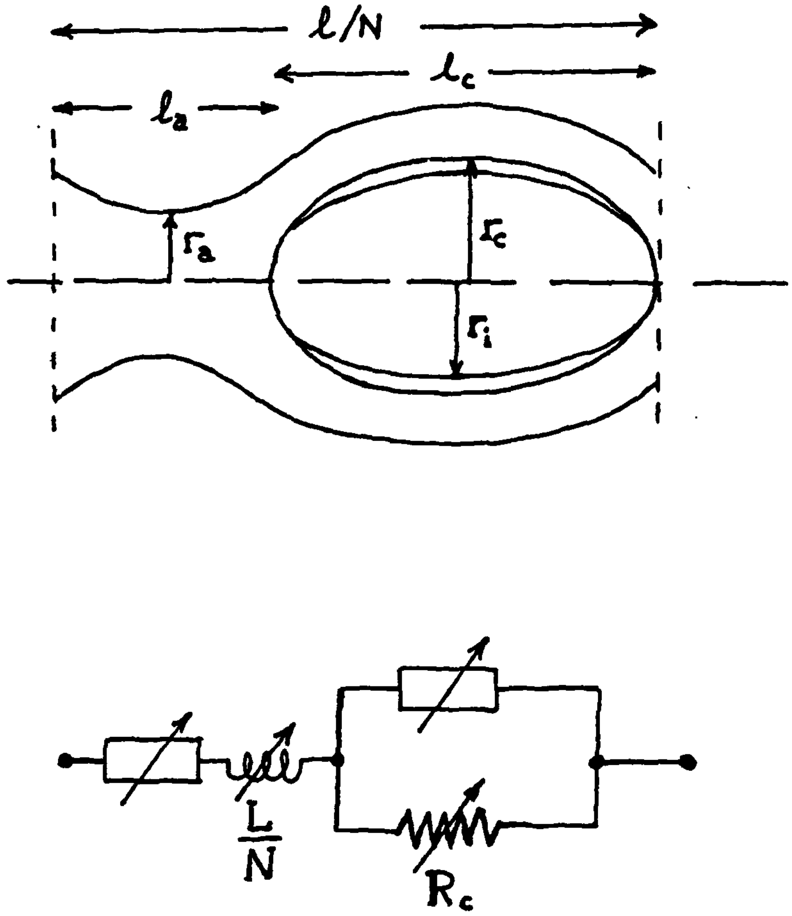

Fig. 1. Geometry and circuit model for one element of a beaded discharge. Rectangular boxes signify current limiters.

JOULE HEATING

Setting aside for now the question of inductive corrections, this allows us to estimate the Joule heating rate in the anomalous regions in the DC case:

$$E \cdot I = \frac{VI}{N_a \ell_a} - \frac{N_c \ell_c}{N_a \ell_a} R_c I^2 \qquad (6)$$

where the last term is neglected and where I is given by Eq. (4). If all this energy went into electron temperature and none escaped to ions or photons, it would correspond to a rise

$$\dot{T} = \frac{2}{3} \frac{VI}{N_a \ell_a} \frac{1}{\pi r_a^2 \, z n_i} \qquad (7)$$

$$\text{i.e., } \dot{T}(\text{keV/ns}) \approx 15 \; V(\text{MV}) \left[\frac{1}{N_a \ell_a(\text{cm})}\right] \left(\frac{26}{A} \; \frac{z}{10}\right)^{\frac{1}{2}} T_{keV}^{\frac{1}{2}} \;, \qquad (8)$$

a number of order 15 keV/ns.

The transit time of a typical electron from one bead to the next at a constant sound speed $c_s(T_{keV})$ would be

$$\tau = \ell_a/c_s = 4.5 \times 10^{-9} \text{ sec} \times \ell_a(\text{mm}) \left(\frac{A}{26} \; \frac{10}{z}\right)^{\frac{1}{2}} T_{keV}^{-\frac{1}{2}} \qquad (9)$$

or a few ns, so that an electron could acquire several tens of keV before plowing into the adjacent dense bead and losing its energy to dense-plasma thermal energy and not-so-cold-target bremsstrahlung. In fact, a certain amount of this energy is lost to ions and radiation during transit across the anomalous region, and we now give estimates showing that loss to be dominated by classical heat conduction.

COOLING RATES OFFSETTING JOULE HEATING

The classical collisional electron cooling time to ions of atomic mass A (taken from Book, 1980) is

$$\dot{T}(\text{keV/ns}) \approx -3.6 \times 10^{-2} \left(\frac{z}{10}\right)^2 \left(\frac{\ln\Lambda}{10}\right) \left(\frac{26}{A}\right) \left(\frac{n_e}{10^{19}}\right) T_{keV}^{-1/2} \tag{10}$$

which is negligible at 1 keV and above (unless $n_e > 10^{21}\ \text{cm}^{-3}$). The radiative cooling gives approximately

$$\dot{T}(\text{keV/ns}) \sim -4.4 \times 10^{-2}\ T_{keV}^{-1} \left(\frac{n_i}{10^{18}}\right)^{3/2} \tag{11}$$

for aluminum with $T_e \geq 1$ keV (Terry and Guillory, 1980b, p. 5 and plasma radiation transport computations done by Duston (1980)).

The classical heat flux, which is dominated by the Hall flux term $\hat{B} \times \nabla_\perp T_e$ since ν_e/ω_{ce} is small except very near the axis, would give a cooling rate

$$\dot{T}(\text{keV/ns}) \sim -3.5 \times 10^{-2}\ \frac{r_a}{r_T} \left(\frac{A}{26}\right)^{1/2} \left(\frac{10}{z}\right)^{3/2} \left(\frac{10^{18}}{n_i}\right) \left(\frac{1\ \text{mm}^2}{\pi r_a^2}\right) T_{keV}^{3/2} \tag{12}$$

where r_T is the radial temperature scaleheight.

The modified two-stream instability (Krall and Liewer, 1971; Ott et al, 1972) grows at a rate about half the lower-hybrid frequency

$$\omega_{LH} = \sqrt{\omega_{ce}\omega_{ci}} \sim 6 \times 10^{11} \left(\frac{26}{A}\right) \left(\frac{z}{10}\right)^2 \left(\frac{n_i}{10^{18}}\right)\left(\frac{r_a}{1\ \text{mm}}\right) T_{keV}^{1/2} \tag{13}$$

(based on Eq. (4) for I) and thus can easily saturate in less than 1 ns, leading to alteration of the diffusive heat flux as well as being the source of the drift-speed limiting assumed at the outset.

But the alteration of the heat flux, according to the form of anomalous heat conductivity given by Manheimer (1979),

$$\kappa \sim cT/16\ eB \tag{14}$$

is small and gives a contribution

$$\dot{T}(\mathrm{keV/ns}) \sim 10^{-3} \left(\frac{A}{26}\right)^{\frac{1}{2}} \left(\frac{10}{z}\right)^{3/2} \left(\frac{10^{18}}{n_i}\right) \left[\frac{r(\mathrm{mm})}{\pi r_a^2(\mathrm{mm}^2)\,\ell^2(\mathrm{mm}^2)}\right] T_{\mathrm{keV}}^{-3/2} \tag{15}$$

to the electron cooling in transit across the anomalous low-density regions. (The inverse dependence on n_i comes only from the linear dependence of I, and thus B, on n_i.)

The instability tries to stabilize by bringing a small number of ions up to the sound speed (Vekshtein et al, 1971) but this is an important energy drain for the electrons only where $T_e >> T_i$. [For the time development of T_i due to this anomalous heating, one may consult Lampe et al, (1971)]. A fraction $f_i \sim (m_e/m_i)^{\frac{1}{4}}$ of the ions is accelerated to a speed comparable with c_s, i.e., to energies $\frac{3}{2} T_e$. (The directions are isotropized by the magnetic field.) There is thus a net loss of ion thermal energy due to the exit of these particles from the low density region, which is only partly compensated by the thermal influx of ions at temperature T_i. The net heat loss flux per cm^2 of area is

$$n_i f_i \left[\left(\frac{1}{4}\, c_s\right)\left(\frac{3}{2}\, T_e\right) - \left(\frac{1}{4}\, v_{Thi}\right)\left(\frac{3}{2}\, T_i\right)\right] \tag{16}$$

(v_{Thi} is the ion thermal speed); and when the instability is saturated and quasi-steady this energy loss is made up by energy transfer from electrons to ions via unstable waves:

$$\frac{3}{2}\, n_e \dot{T}_e\, \pi r_a^2\, \ell a = \pi r_a^2 \left(\frac{3}{8}\, n_i f_i\right)\left[c_s T_e - v_{Thi}\, T_i\right] \quad .$$

This gives rise to an electron cooling rate

$$\dot{T}_e(\text{keV/ns}) \leq .5 \times 10^{-3} \left(\frac{10}{z}\right)^{\frac{1}{2}} \left(\frac{26}{A}\right)^{3/4} \left(\frac{1\ \text{mm}}{\ell_a}\right) T_{\text{keV}}^{3/2} \quad . \tag{17}$$

This rate is small because of the small number of ions involved, relative to the number of electrons. In fact, for nominal parameters all of the electron cooling rates (10) - (17) are small compared with the Ohmic heating rate, and so most of the Ohmic energy gain is delivered to the blobs after transit across the anomalous region.

POWER DELIVERY

Assuming the dense blobs to the thicker than one range for the 15-50 keV electrons accelerated into them, the total net power delivery to them is

$$P \sim \frac{3}{2} (T_e - T_{eo})\, N\pi r_a^2\, n_e c_s \tag{18}$$

where $T_e - T_{eo}$ is the temperature gain by Ohmic heating, less losses, during transit from blob to blob. If the cooling during transit is negligible and if almost all the voltage drop occurs across the low-density regions, then the power delivered is

$$P(TW) = 0.36 \left(\frac{V}{1MV}\right) \left(\frac{\pi r_a^2}{1\ mm^2}\right) \left(\frac{z}{10}\right)^{3/2} \left(\frac{26}{A}\right)^{\frac{1}{2}} \left(\frac{n_i}{10^{18}}\right) T_{keV}^{\frac{1}{2}} \tag{19}$$

with n_i, T_{keV} representing either their average values of their initial (unheated) values in the low-density region. If less than the full voltage drop occurs across the anomalous regions, the value of V above is adjusted downward accordingly.

PEAK ELECTRON TEMPERATURE

In the low-density regions, the electron temperature varies axially, increasing in the direction of electron flow because of collisional and unstable-wave isotropization of the energy gained from the axial electric field. The temperature begins at approximately its value in the adjacent classical bead (a quasi-balance of deposition and radiative loss), increases as the electron traverses the low density region, and reaches its maximum just before deposition i the next "bead" downstream.

Since the heating during transit has the approximate form $\dot{T}_e \propto T_e^{1/2}$ (from Eq. (8)), one has for the case of negligible heat conduction and radiation

$$\left.\begin{aligned} c_s(t) &\approx c_s(0) + \dot{c}_s t \\ \dot{z}(t) &= c_s(t) \end{aligned}\right\} \qquad (20)$$

So that $z(t) = \dot{c}_s(0)t + \frac{1}{2}\, c_s t^2$ and the final temperature is such that

$$c_s(t_f) = \sqrt{c_{so}^2 + 2\, \dot{c}_s \ell_a} \qquad (21)$$

i.e. $$T_e(\ell_a) = T_{eo} + \frac{670\ \text{keV}}{N_a}\left[V(\text{MV}) - L\dot{I}\right] \qquad (22)$$

from Eqs. (3) and (8), as an overestimate of the peak temperature. (N_a, the number of anomalous regions, is observed to be typically of the order of 20 to 30, while the inductively corrected voltage V - LI is one or two MV.) The voltage drop along the classical beads has been neglected compared with that over the anomalous regions between beads, and including it reduces the effective voltage appearing in Eq. (22) to that occurring only over the N_a anomalous regions. In this approximation the temperature increases linearly with distance across each acceleration region.

The indication that the peak electron temperature may be tens of keV implies that Bremsstrahlung and inner shell x-rays can be produced, predominantly on the cathode ends of the classical beads if their density is high enough, or throughout the beads if they are only about one range thick for the energetic electrons.

INDUCTIVE EFFECTS

The generalized Ohm's law in a classical medium takes the form

$$E = \eta J + k\dot{J} - \frac{v}{e} \times B \qquad (23)$$

or $$V = RI + L\dot{I} + \dot{L}I \quad . \qquad (24)$$

(k is a constant related to the electron inertia and the geometry, and L is the self-inductance.) Voltages induced by changing the current-carrying radius r_a are of order

$$E(\mathrm{MV/cm}) \sim 2I(\mathrm{MA}) \frac{\dot{r}_a}{r_a} (\mathrm{ns}^{-1}) \ , \qquad (25)$$

which becomes of .rder 1 MV just before the peak compression. The corresponding impedance

$$\dot{L}\ (\mathrm{Ohms}) \sim 2\ell(\mathrm{cm})\ \dot{r}_a/r_a\ (\mathrm{ns}^{-1}) \qquad (26)$$

has maximum value on the order of 1 Ohm, in series with 1-4 Ohms effective resistance, and so is not a negligible correction except for a few-nanosecond intervals when $\dot{r}_a \approx 0$. In SPLAT code runs, the $\dot{L}$ term is even somewhat larger, at its maximum, than the Ohmic resistance of the classical plasma core. But where the current becomes limited by anomalous regions in series with classical ones, the effective resistance R* in the equation

$$V = R^*I + L\dot{I} + \dot{L}I \qquad (27)$$

is larger (and voltage-dependent, as V); so the $\dot{L}$ term no longer <u>dominates</u>, although it is not strictly negligible except very near peak compression and for the "pause" phase of "pause-and-collapse" compressions. For our simple description we neglect the $\dot{L}$ term, which is acceptable when V/I is much larger than $\dot{L}$, i.e.,

$$\frac{r_a}{r_a}\,(\mathrm{ns}^{-1}) \ll 1.4\,\frac{V(\mathrm{MV})}{\ell(\mathrm{cm})}\left(\frac{A}{26}\right)^{1/2}\left(\frac{10}{z}\right)^{3/2}\left(\frac{10^{18}}{n_i}\right)T_{\mathrm{keV}}^{-1/2}\left(\frac{1\ \mathrm{mm}^2}{\pi r_a^2}\right) \tag{28}$$

The $L\dot{I}$ term may be governed by nonlinear sausage instability dynamics not yet well understood; when I is given by Eq. (4), I is proportional to $\frac{d}{dt}(n_i \pi r_a^2)$, i.e., the change in particle number in the necked-off region. This subject is to be investigated uner 1981 and 1982 funding, and is beyond the scope of available theory at the time of this report.

JUSTIFICATION OF DRIFT-SPEED-LIMITED CURRENT

When the ion and electron temperatures are comparable one does not get appreciable growth of the ion acoustic instability (Kovrizhnykh, 1967; Biskamp and Chodura, 1971), but the modified two-stream instability (Ott et al, 1972; McBride et al, 1972) grows with linear growth rate

$$\mathrm{Im}\ \omega(\mathrm{MTS}) \sim \frac{1}{2}\,\omega_{LH} = \frac{1}{2}\,\omega_{pi}(1 + \omega_{pe}^2/\omega_{ce}^2)^{-1/2} \approx \frac{1}{2}\,\omega_{ce}\sqrt{A/Z} \qquad (29)$$

where ω_{LH} is the "lower hybrid" frequency, ω_{pe} is the plasma frequency, and ω_{ce} is the electron gyrofrequency. This persists as long as the drift velocity v_d exceeds approximately the sound speed, c_s, and is marginally stable when $v_d \approx c_s$. The nonlinear saturation time, of order 300 ω_{pe}^{-1}, is much shorter than the ℓ/c_s transit time of electrons across the anode-cathode gap, so the waves can grow to saturation within the diode.

Including the electron magnetization more carefully, one also gets an "electron cyclotron drift instability" (Forslund, Morse and Nielsen, 1972)with growth rate

$$\mathrm{Im}\ \omega(\mathrm{ECD}) \sim \omega_{ce}\,\frac{v_d}{v_e}\,\frac{T_e}{2T_i} - \nu_{ei} \qquad (30)$$

where v_d is the electron drift speed, v_e is the electron thermal speed, and ν_{ei} the electron collision frequency as before. But for typical parameter values, v_d/v_e should be of order $\sqrt{A/Z}$ so the two linear growth rates are comparable:

$$\mathrm{Im}\ \omega \sim 2.6 \times 10^{11} \left(\frac{z}{10}\,\frac{26}{A}\right)^{1/2} \frac{I(\mathrm{MA})}{r_a(\mathrm{mm})} \qquad (31)$$

as long as this exceeds ν_{ei} in Eq. (1).

The radial gradients in magnetic fields can also give rise to a "lower-hybrid drift" instability (Krall and Liewer, 1971) with linear growth rate

$$\text{Im } \omega(\text{LHD}) \sim \omega_{pi}\left[\frac{1}{2B}\frac{dB}{dr}\frac{v_e^2}{\omega_{ce}\, c_s}\right]^{\frac{1}{2}} (\omega_{ce}/\omega_{pe})$$

$$\sim 7.4 \times 10^{-5}\ \omega_{ce}\left[\frac{26}{A}\left(\frac{10}{Z}\right)^3 \frac{T_{keV}}{h_B^2 B(MG)^2}\right]^{1/4}$$

where $h_B = \left(\frac{1}{B}\frac{dB}{dr}\right)^{-1} \sim r_a(\text{cm})$.

Since B is at most $2I/cr_a$, this gives

$$\text{Im } \omega(\text{LHD}) \leq 10^{10}\ \frac{I_{MA}^{\frac{1}{2}}}{r_a(\text{mm})}\left[\left(\frac{26}{A}\right)\left(\frac{10}{Z}\right)^3 T_{keV}\right]^{1/4}\left(\frac{r_a}{h_B}\right)^{1/2} \qquad (32)$$

which is generally less than the MTS and ECD instability growth rates.

Because the modified two-stream instability exponentiates in a few picoseconds and saturates in several growth times, it is most likely that the electron drift speed is limited in this way to values near that which stabilizes the instability, namely the sound speed. This is the justification for the anomalous drift-speed-limited current-carrying behavior assumed earlier.

APPLICATION TO CYLINDRICAL IMPLOSIONS AND THE "SPLAT" CODE

From Eqs. (2) and (3), we easily derive a fact of some significance. Before the field has penetrated a cylindrical z-pinch plasma, the radial profile of the E_z electric field of course goes from negligible values at the current penetration front to values of order V/ℓ at large radii. For all radii where

$$E(r)\ (\mathrm{MV/cm}) > \left(\frac{.12}{T_{keV}}\right)\left(\frac{n_i(r)}{10^{20}}\right)\left(\frac{26}{A}\right)^{\frac{1}{2}}\left(\frac{\ell n\Lambda}{10}\right)\left(\frac{z}{10}\right)^{5/2}, \tag{33}$$

the current is drift-speed limited. For temperatures of order $\frac{1}{2}$ keV and above, the critical E(r) value at r=a is much less than $V/\ell \sim 1\mathrm{MV/cm}$ when $n_i(r)$ is small compared with 10^{20}.

But from the voltage rise time $\tau_v \sim 10^{-7}$ sec, we can estimate a classical skin depth in the dense (classical) region:

$$\Delta(\mathrm{cm}) = 29\sqrt{\tau_v(\mathrm{sec})}\ T_{keV}^{-3/4}\left(\frac{\ell n\Lambda}{10}\,\frac{z}{10}\right)^{\frac{1}{2}}, \tag{34}$$

and this gives a core current,

$$I_1 = \int_0^a 2\pi r\sigma E(a)e^{-(a-r)/\Delta}dr,\ \text{i.e.,}$$

$$I_1(\mathrm{MA}) = 0.21\left(\frac{\tau_v}{10^{-7}}\right)^{\frac{1}{2}}\left(\frac{z}{10}\right)^2 T_{keV}^{-1/4}\left(\frac{\ell n\Lambda}{10}\right)^{\frac{1}{2}}\left(\frac{26}{A}\right)^{\frac{1}{2}} a(\mathrm{mm})\,\frac{n_i(a)}{10^{18}} \tag{35}$$

When the core carries most of the current ($I \approx I_1$), this gives for the density at the critical surface of radius a

$$\frac{n_i}{10^{18}} = 4.8\left(\frac{10}{\ell n\Lambda}\,\frac{A}{26}\right)^{\frac{1}{2}}\left(\frac{10}{z}\right)^2 T_{keV}^{\frac{1}{4}}\left(\frac{10^{-7}}{\tau_v}\right)^{\frac{1}{2}}\frac{I(\mathrm{MA})}{a(\mathrm{mm})} \tag{36}$$

Thus, for a keV aluminum plasma carrying 1 MA current at the skin of a 1 mm^2 area, if the on-axis density drops below about 10^{19} ions/cm^3 anywhere, then the classical "core" tends to disappear there. And since this value (Eq. 36) of n_i tends to be small compared with 10^{20} cm^{-3}, most of the E field is shielded from the classical region, i.e., $E(a) << V/\ell$, while there is a classical region.

The one-dimensional strongly-coupled plasma implosion code SPLAT (Terry and Guillory, 1980b), sets (initially) a radius a beyond which the current is drift speed limited at the initial temperature. In the present form of the code, this radius is then followed in a Lagrangian manner, moving with the fluid velocity. In fact, however, as the temperature and current increase, the real "critical surface" at which conduction becomes anamalous moves inward more rapidly than the particles, following the variable density contour of Eq. (36). Thus a larger and increasing fractionof the current, I_2/I, is carried "anomalously." This fraction is thus underestimated by the code. The corona is actually more important than indicated by the code for another reason: its density at the true "critical surface" r=a is larger than presently accounted for and the total ohmic heating should be larger.

SAUSAGE INSTABILITY DYNAMICS

The nonlinear behavior of the axisymmetric sausage instability has been treated only in a few limiting cases. A nonradiating, perfectly conducting incompressible MHD model with uniform density and no heat conduction was treated by Book, Ott and Lampe (1976). In both the long wavelength ($\lambda >> r$) and short wavelength limits, these assumptions gave tractable equations, which showed a spool-like development of the plasma shape, with thin rapidly expanding disks of enlarged radius and broad, slowly constricting regions of reduced radius. The presence of finite conductivity and axial electric field certainly modifies the dynamics; and even more so, the inclusion of finite compressibility, which is being studied now by Book et al, may greatly alter the conclusions made in the simpler model.

Because of this, we have proposed in our 10/81-10/82 program an extension of the Book et al theory to include finite conductivity and E field, and the construction of a 2-dimensional r-z code for modeling the behavior with radiation, circuit model, etc. coupled into the dynamics.

The equations describing the motion are:

continuity: $\partial_t \rho + \partial_z(\rho v_z) + \frac{1}{r}\partial_r(\rho r v_r) = 0$

$\rho D\vec{v}/Dt = \nabla P$: $\rho(\partial_t v_z + v_z \partial_z v_z + v_r \partial_r v_z) = -\partial_z P$

$$\rho(\partial_t v_r + v_z \partial_z v_r + v_r \partial_r v_r) = -\partial_r P \tag{37}$$

state: $P = \gamma T \rho / m_i + B^2/8\pi + KB^2/r \qquad B^2 = B^2(r,z)$

$\nabla x B$: $\frac{1}{r}\partial_r(rB) = \frac{4\pi}{c} J_z; \quad -\partial_z B = \frac{4\pi}{c} J_r$

$\nabla x E$: $\partial_z E_r - \partial_r E_z = -\frac{1}{c}\partial_t B$

$\nabla \cdot J = 0$: $\frac{1}{r}\partial_r (r J_r) + \partial_z J_z = 0$

Ohm's Law:

$$J_z = \mathrm{Min}\left\{\frac{\rho}{m} z k_J T^{\frac{1}{2}},\ \left\{k_\sigma T^{3/2}\left(E_z + \frac{v_r}{c}B\right)\left(1 + \frac{k_\sigma^2 T^3 B^2}{k_B^2 \rho^2}\right)^{-1}\right.\right.$$

$$\left.\left. + k_B \rho T^{-3/2}\left(\frac{E_r}{B} - \frac{v_z}{c}\right)\left(1 + \frac{k_B^2 \rho^2}{k_\sigma^2 T^3 B^2}\right)^{-1}\right\}\right\}$$

$$J_r = \mathrm{Min}\left\{\frac{\rho}{m} z k_J T^{\frac{1}{2}},\ \left\{k_\sigma T^{3/2}\left(E_r - \frac{v_z B}{c}\right)\left(1 + \frac{k_\sigma^2 T^3 B^2}{k_B^2 \rho^2}\right)\right.\right.$$

$$\left.\left. + k_b \rho T^{-3/2}\left(\frac{E_z}{B} + \frac{v_r}{c}\right)\left(1 + \frac{k_B^2 \rho^2}{k_\sigma^2 T^3 B^2}\right)^{-1}\right\}\right\}$$

Heat balance: T specified as function of discharge voltage and ρ, in simplest model, or governed by time dependent heating and cooling rates, in more complex model.

The radial component of J cannot be neglected because then $\partial_z B=0$ does not allow the instability. The constants k_σ in the unmagnetized conductivity and k_B in the Hall conductivity can be found in the standard textbooks; the constant k_J (see Eq. (4)) gives the drift-speed limited current. The constant K provides the magnetic hoop stress due to B-line curvature. The mass density is denoted by ρ, electron (and ion) temperature by T, and fluid velocity by (v_r,v_z). All field and fluid quantities are functions of r and z. Imposing self-similar convex profiles of ρ with radius (e.g., Bennett profiles) and periodicity in z, with only the on-axis density and Bennett radius varying in z, may allow certain artificial but useful simplifications. Making the ideal-MHD assumption is not admissible here, as it allows only surface currents and cannot predict the density drop in the necked-off regions. The fluid model described may break down when these regions produce non-stagnated electron flows.

REFERENCES

Biskamp, D. and R. Chodura, "Computer Simulation of Anomalous Resistance," Phys. Rev. Lett. 27, 1553 (1971).

Book, D. L., 1980 Revised NRL Plasma Formulary. Naval Research Laboratory, 1980.

Book, D. L., E. Ott, and M. Lampe, "Nonlinear Evolution of the Sausage Instability," Phys. Fluids 19, 1982 (1976).

Forslund, D. W., R. L. Morse, and C. W. Nielson, "Nonlinear Electron-Cyclotron Drift Instability and Turbulence," Phys. Rev. Lett. 27, 1424 (1971).

Goldstein, Shyke, in H. W. Bloomberg, et al., "Energy Coupling Mechanisms in Multiple Wire Array Configurations," Science Applications, Inc. Report #SAI-102-72-004, (1979).

Kovrizhnykh, L. M., "Nonlinear Theory of Current Instability in a Non-isothermal Plasma," Sov. Phys. JETP 24, 1210 (1967).

Krall, N. A. and P. C. Liewer, "Low-Frequency Instabilities in Magnetic Pulses," Phys. Rev. A4, 2094 (1971).

Lampe, M., W. M. Manheimer, J. B. McBride, J. H. Orens, R. Shanny and R. N. Sudan, "Nonlinear Development of the Beam-Cyclotron Instability," Phys. Rev. Lett. 26, 1221 (1971).

Manheimer, W. M., "Anomalous Transport from Plasma Waves," Journal de Physique, 40, C7-269 (1979) Suppl.;

McBride, J., E. Ott, J. Boris, and J. Orens, "Theory and Simulation of Turbulent Heating by the Modified Two-Stream Instability," Phys. Fluids 15, 2367 (1972).

Ott, E., J. B. McBride, J. H. Orens, and J. P. Boris, "Turbulent Heating in Computer Simulations of the Modified Plasma Two-Stream Instability," Phys. Rev. Lett. 28, 88 (1972).

Terry, R. E., and J.Guillory, "Development and Exploration of the Core-Corona Model of Imploding Plasma Loads." JAYCOR Report No. TPD200-80-001-FR, July 1980.

Terry, R. E., and J.Guillory, "Semi-Annual Report on Modeling of the Coupling of Imploding Wire Arrays to High-Voltage Generators." JAYCOR Report No. TPD200-80-012, October 1980.

Vekshtein, G. E., D. D. Ryutov and R. Z. Sagdeev, "Asymptotic Solution of the Problem of the Anomalous Resistance of a Collisionless Plasna," Sov. Phys. JETP 33, 1152 (1971).